INTERNATIONAL
Agrophysics
www.international-agrophysics.org

Int. Agrophys., 2026, 40, 95-114
doi: 10.31545/intagr/213794

Landscape elements as windbreaks and their influence on microclimatic parameters in a semi-arid agricultural site in Central Europe**

Günther Gollobich[1]*, *Josef Eitzinger*[2], *Juergen Friedel*[3], *Helmut Wagentristl*[4], *Philipp Weihs*[2], *Karl Gartner*[1], *Aliyeh Salehi*[3]

[1]Department of Forest Ecology and Soil, Subdivision Site and Vegetation, Austrian Research Centre for Forests (BFW) Seckendorff-Gudent-Weg 8, 1130, Vienna, Austria
[2]Institute of Meteorology and Climatology (BOKU-MET), BOKU University, Gregor-Mendel Straße 33, 1180, Vienna, Austria
[3]Institute of Organic Farming (IFÖL), BOKU University, BOKU University, Gregor-Mendel Straße 33, 1180, Vienna, Austria
[4]Experimental Farm, Groß-Enzersdorf, Boku University, Schloßhofer Straße 31, 2301, Groß-Enzersdorf, Austria

Received June 13, 2025; accepted October 31, 2025

A b s t r a c t. In the semi-arid regions of Eastern Austria, windbreaks are essential for reducing wind velocity (*WV*) and grass reference and actual evapotranspiration (Et_0, Et_a), thereby influencing yields. This case study examines the effects of two windbreak systems: 1) a hedgerow-based wind protection system (WPS) and 2) a strip intercropping experiment (SICE) with variable row widths in a maize-soybean intercropping setup. Micrometeorological data were collected at both sites, including wind velocity, wind direction, air temperature, global radiation, and relative humidity at multiple heights. The WPS reduced wind velocity by 0.8-1.1 m s^{-1} (2 m height) and 0.6-0.8 m s^{-1} (1 m height) leeward of the hedge compared to a 10 m reference height. At the SICE, reductions ranged from 0.1-1.2 m s^{-1} (2 m) and 0.2-0.5 m s^{-1} (1 m). Relative wind reduction effects (WRE) reached 34-41% (WPS) and 31-56% (SICE). A hedgerow coefficient (Δf) was used to standardize the WRE by hedgerow height and distance in different systems. Et_0 decreased by 0.6-0.7 mm d^{-1} near the WPS, while Et_a rose by 0.2-0.5 mm d^{-1} due to improved water availability. At the SICE, Et_0 increased by 0.9-1.7 mm d^{-1}, and Et_a showed varied responses. Overall, windbreaks can enhance water use efficiency and support sustainable landscape design in semi-arid agriculture.

K e y w o r d s: evapotranspiration, wind reduction, agrometeorology, hedgerow, adaptation measure, crop microclimatic conditions

1. INTRODUCTION

Two different windbreak systems include hedgerow-based systems: wind protection systems (WPSs) and a crop-based system: strip intercropping experiment (SICEs). WPSs such as hedgerows play a crucial role in agriculture by reducing wind velocity (*WV*) and positively influencing water retention and evapotranspiration rates (Et_0, Et_a). They also influence other microclimatic parameters like air temperature (*AT*), relative air humidity (RH), and global radiation (*GR*) in adjacent agricultural production areas (Böhm *et al.*, 2014; Bitog *et al.*, 2012; Vacek *et al.*, 2018). In crop-based systems, unlike hedge-based WPSs, microclimatic parameters (Et_0, Et_a, *WV*, *AT*, *RH*, *GR*) are also affected (Jurik *et al.*, 2004). However, the main focus in most studies is primarily wind erosion. Currently, there are no studies addressing the effect of wind reduction, and relevant studies only involve strip intercropping combined with existing hedge-based WPSs. Furthermore, they do not focus on the interactions within the rows of the strip intercropping system and the influence on microclimatic parameters.

*Corresponding author e-mail: guenther.gollobich@bfw.gv.at
**The BOKU University provided the submission fee for the article.

In conventional farming, high *WV* and drought conditions can cause significant damage to young plant parts, leading to dehydration and reduced yields (Stahr, 2017). Additionally, unproductive water losses result from wind exposure, which are coupled with an increasing frequency of dry periods in recent decades, particularly in the Marchfeld in Eastern Austria, which poses a serious challenge to sustainable agriculture and often necessitates costly irrigation investments (Weninger *et al.*, 2021; Campi *et al.*, 2009). The effectiveness of WPSs largely depends on their structural characteristics, including ventilation properties (well-ventilated, poorly ventilated, or non-ventilated) (Wendt, 1951; Campi *et al.*, 2012). A WPS not only reduces *WV* but also modifies the microclimate in its vicinity (Sudmeyer *et al.*, 2007). For instance, shading effects and decreased *WV* near the WPS can lead to increases in near-ground air temperatures (0.02 m) compared to the surrounding environment (Wendt, 1951).

A similar effect has been observed in soil moisture levels throughout the growing season (Weninger *et al.*, 2022; Ableidinger *et al.*, 2020). Seeds in the sheltered range of a WPS germinate faster and grow more vigorously than those outside this range as they can utilize soil moisture more efficiently. Consequently, in drought conditions, yields in protected areas tend to be higher and more stable (Radke *et al.*, 1976).

WPSs also promote the nightly condensation of atmospheric moisture, leading to increased dew formation near hedgerows, which is an important factor for crop yields, especially in dry years (Wendt, 1951). As a result, WPSs contribute to higher and more stable crop production (Gagarin, 1949; Cleugh, 1998; Thevs *et al.*, 2017). Additionally, they help to regulate the microclimate by mitigating extreme weather conditions, improving soil structure, and reducing both wind and water erosion (Ableidinger *et al.*, 2018; Gerersdorfer *et al.*, 2010). Almost all microclimate variables are altered in the leeward zone of a WPS, with shading affecting a narrow area adjacent to the barrier (Forman and Baudry, 1984). However, wind remains the dominant factor that controls microclimate variability (Heisler *et al.*, 1988).

Compared to open fields, areas protected by WPSs experience increased daytime and nighttime temperatures, higher soil temperatures, enhanced dew formation, and elevated atmospheric moisture, while *WV* and evapotranspiration rates (Et_0, Et_a) are generally lower. WPS effects can extend over distances of 10-16 times the barrier height for evaporation and up to 28 times the hedgerow height for *WV* reduction (Forman and Baudry, 1984). Beyond their role in modifying local microclimates, WPSs also support biodiversity by facilitating species migration and persistence due to stable temperature conditions. This thermal buffering effect may become increasingly important in the context of climate change (Vanneste *et al.*, 2020). Studies show similar effects in decreasing evapotranspiration rates (Et_0, Et_a) in comparable fields (Veste *et al.*, 2020).

WPSs are key structural elements in rural landscapes that contribute to soil conservation, biodiversity enhancement, and pest control (Weninger *et al.*, 2021; Brandle *et al.*, 2004). However, their impact on biomass production, nutrient cycling, and water balance can vary, with some studies reporting positive effects, while others indicate neutral or even negative outcomes (Řeháček *et al.*, 2017; Weninger *et al.*, 2021). *WV* reductions on the leeward side of WPSs increase with distance, typically reaching values between 9.7 and 15% (Weninger *et al.*, 2021; Vacek *et al.*, 2018; Miri *et al.*, 2021). Some studies report reductions of up to 50% (Böhm *et al.*, 2014), 78% (Dufkova, 2007), and a maximum of 85% at 1 barrier height (Peri *et al.*, 2002).

Many different studies have examined WPSs effects of specific systems, like WPSs and SICE, but there are hardly any systematic studies analyzing and comparing the effects of different WPS types in the same environmental conditions. Therefore, the aim of this case study was to analyze two distinct systems that are most commonly applied-hedgerow-based and crop-based systems-in order to find a method for upscaling their effects for a larger landscape. In this context, we addressed the following key research questions: a) What are the differences in wind-reduction effects in the protected areas between two common windbreaks (WPS, SICE) of different type and height? b) To what extent do the calculated evapotranspiration rates (Et_0, Et_a) differ between these two windbreak types? c) Can a hedgerow coefficient (Δf) be defined and used for spatial upscaling of windbreak effects?

2. METHODS

2.1. Site characteristics and measurement setup of the first site (WPS*)*

The observed WPS is located east of Vienna (48.207356, 16.62617, decimal degrees, WGS 84) in the agricultural main production area known as the "Marchfeld." The site is situated at an altitude of 156 m a.s.l. and features flat topography. The hedgerow is oriented north-northeast (19°) (Fig. 1a, b, Fig. 2) and has a total length of 600 m. It was divided into two intensively monitored subareas: windward (LUV) and leeward (LEE) with respect to the prevailing wind direction (WD) and long-term measurements (agrometeorological weather station).

The hedge comprises the following deciduous tree and shrub species: *Acer campestre, Acer pseudoplatanus, Cornus sanguinea, Ligustrum vulgare, Prunus mahaleb, Syringa vulgaris, Rosa canina,* and *Robinia pseudoacacia* (Schaufler and Starlinger, 2022, unpub.), which have coverage levels ranging from 1 to 50%. The wind distribution in the observed year of 2021 for LUV and LEE is shown in Fig. 1c, d. The WPS exhibits variable height with a mean of approximately 10 m.

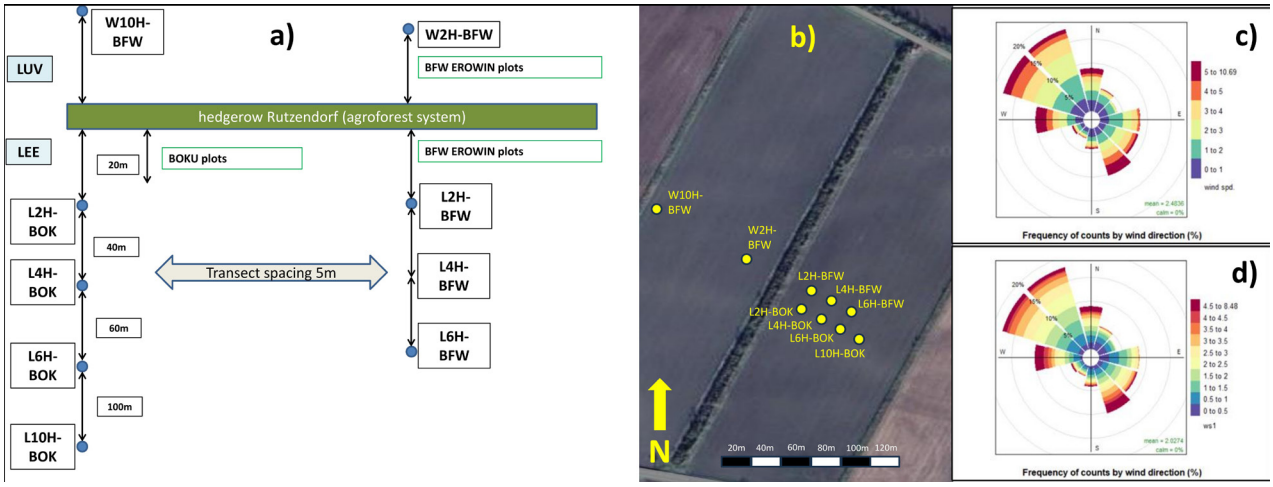

Fig. 1. a) Overview of the observed transects and measuring points in various distances to the WPS; b) overview and orientation of the observed line transects with selected measuring plots leewards: L2H-BOK, L4H-BOK, L6H-BOK, L10H-BOK, L2H-BFW, L4H-BFW, L6H-BFW; windwards: W2H-BFW, W10H-BFW); c) wind velocity distribution according to main geographic direction (N-E-S-W), for the plot L10H-BOK, 2 m measurement height (a.g.l.); d) wind velocity distribution according to main geographic direction (N-E-S-W) for the plot W10H-BFW, 2 m measurement height (a.g.l.), for better visualization of the wind velocity distribution within the figures c and d the wind velocity was distributed into 12 subsectors.

Fig. 2. Leeward side of the WPS System, 15th June 2022.

The subareas were subdivided into four line transects at varying distances from the WPS. The designation of measuring points along these transects is based on multiples of the mean WPS height, with labels 2H-10H corresponding to twofold to tenfold the average WPS height (m) along the horizontal axis (north to south). In the LEE subarea, the horizontal distance between the BOK and BFW line transects is 5 m (Fig. 1b). The BFW transects (LUV, LEE) were established in a previous wind-erosion study (EROWIN; Weninger *et al.*, 2021) and were used to validate measurements obtained near the BOK transect (replications).

2.2. Site characteristics and measurement setup of the second site (SICE)

The observed SICE is located east of Vienna (48.23592, 16.58966, decimal degrees, WGS 84) in the agricultural main production area of the Marchfeld in Eastern Austria. The site is situated at an altitude of 156 m a.s.l. and features flat topography. For microclimatic data collection, two test rows were established, and measurements were conducted in two experimental phases: setup 1 from July 4 to July 28, 2022, and setup 2 from July 28 to October 30, 2022. During both phases, the maize crop was fully developed and reached a stable height of approximately 2 m. Microclimatic measurements were taken at five field stations: a maize reference station (MAIZEREF) located within the 9 m-wide maize strip, a soybean reference station (PEAREF) located within the 6 m-wide soybean strip (Fig. 3), and transect stations within the observed soybean strip at defined distances (H = multiple of maize canopy height of 2 m) from the maize strip (barrier): A0.5H, A1H, and A2H for setup 1 (Fig. 3a-c), and B1H, B2H, and B2.5H for setup 2 (Fig. 3b-d).

2.3. Climate characteristics

In 2003-2024, the mean annual precipitation (MAP) was 538 mm, and the mean annual temperature (MAT) was 11°C. In 2022, the MAT was 12.3°C, and total precipitation (P) was 391 mm, which is 147 mm below the MAP of 560 mm for the reference period of 1991-2020. This precipitation-deficit trend began in 2021, when annual precipitation was 525 mm, which is 35 mm below the long-term mean (LTM) for 2003-2024. The maize and soybean growing season spans May to September (MJJAS). During this period in 2022, the total precipitation was 65 mm, which is slightly below the long-term mean of 66 mm for 2003-2024. The monthly deviations from the LTM during MJJAS 2022 were as follows: May +13 mm, June +17 mm, July +25 mm, August –15 mm, and

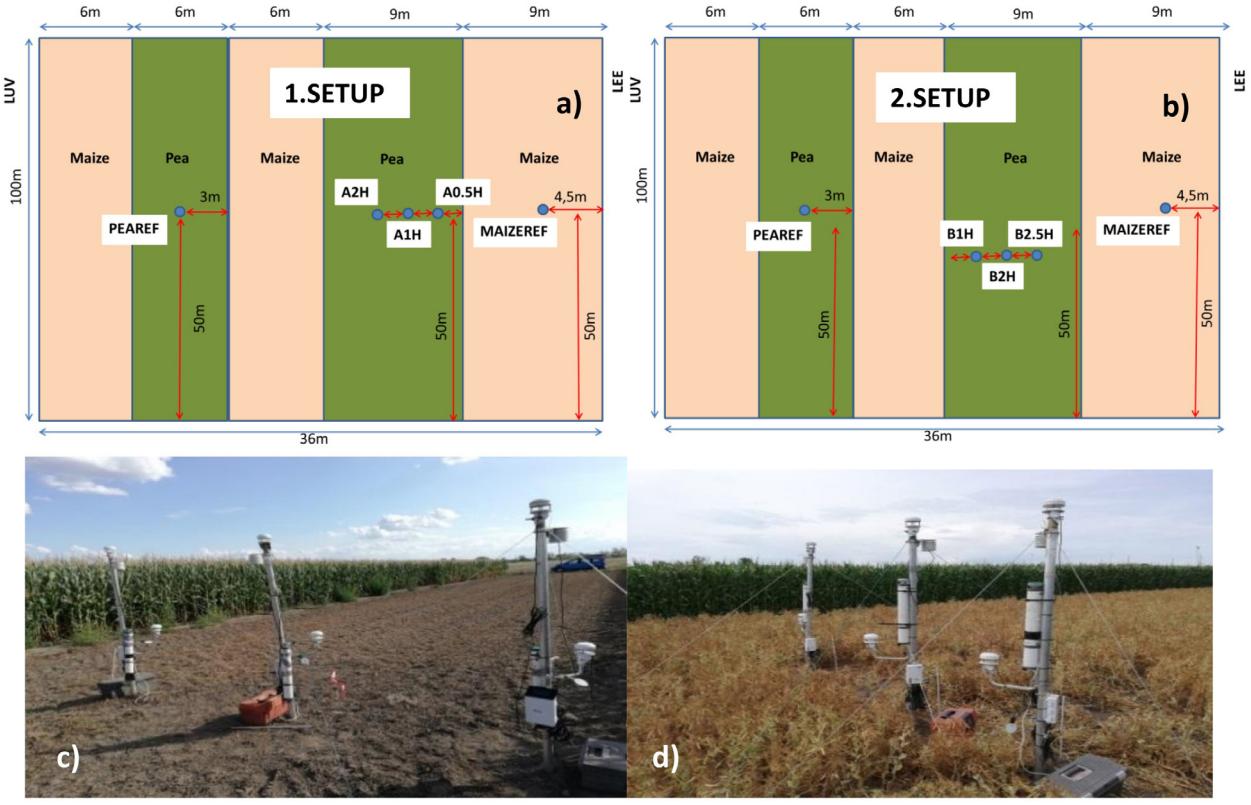

Fig. 3. Map of the SICE experiment 2022 (soybean, maize) with different row widths: a) setup 1 – transect (A0.5H-A2H) leewards within the pea strip; b) setup 2 – transect (B1H-B2.5H) luvwards within the pea strip; c) picture of the leewards transect setup 1 (A0.5H-A2H) within the pea strip; d) picture of the luvwards transect setup 2 (B1H-B2.5H) within the pea strip.

September –20.5 mm. Regarding temperature, the monthly mean temperatures during MJJAS 2022 were higher than the LTM (2003-2024) for all months: May +2.3°C, June +2.4°C, July +0.9°C, August +1.3°C, and September +0.9°C (Fig. 4).

2.4. Soil characteristics

The soils at both WPS and SICE sites are classified as Chernozems according to the WRB (IUSS Working Group WRB, 2022) and developed on calcareous fine sediments (parent material). The soils at the WPS site are dry with low water-storage capacity and high permeability, while at the SICE, they are moderately dry with low storage capacity and moderate permeability. There is a medium level of humus content in the upper horizons (1.5-4%), and the soil is calcareous with a pH of 7.4 at both sites.

The soil horizons at the WPS are A 0-25 cm, A2 40-60 cm, AC 60-70 cm, and C >100 cm, with fractions ranging from loamy silt and sandy loam in the upper horizons to loamy sand and sand in deeper layers. At the SICE, the horizons are A 50-60 cm, AC 70-85 cm, and C up to 120 cm, with loamy sand in the upper horizons and pure sand below 60 cm. According to the Austrian soil map (EBOD2), the area is classified as medium-quality arable land (Aust *et al.*, 2023; www.bodenkarte.at, EBOD2).

2.5. Measured microclimatic and soil variables

Microclimatic measurements were carried out for the WPS site in 2021 and for the nearby SICE site in 2022. A few modifications were made to the measurement set-up due to the different wind-protection systems. At the WPS site (permanent hedgerow), microclimatic variables including *AT*, *RH*, *WV*, *GR*, and *WD* were recorded. The measurement intervals varied according to the sensor and ranged from 1 s to 60 min (Tables 10 and 11).

At the SICE site (maize strip), *AT*, *RH*, *WD*, *WV*, *P*, and *GR* were measured on the PEAREF and MAIZEREF plots (setups 1 and 2). Data were collected during the period when the maize strip acting as a wind barrier had reached its maximum height of approximately 2 m. The temporal resolution of weather stations was 10 min (Tables 12 and 13). During the measurement period, the GR sensor at the PEAREF station was temporarily out of service from

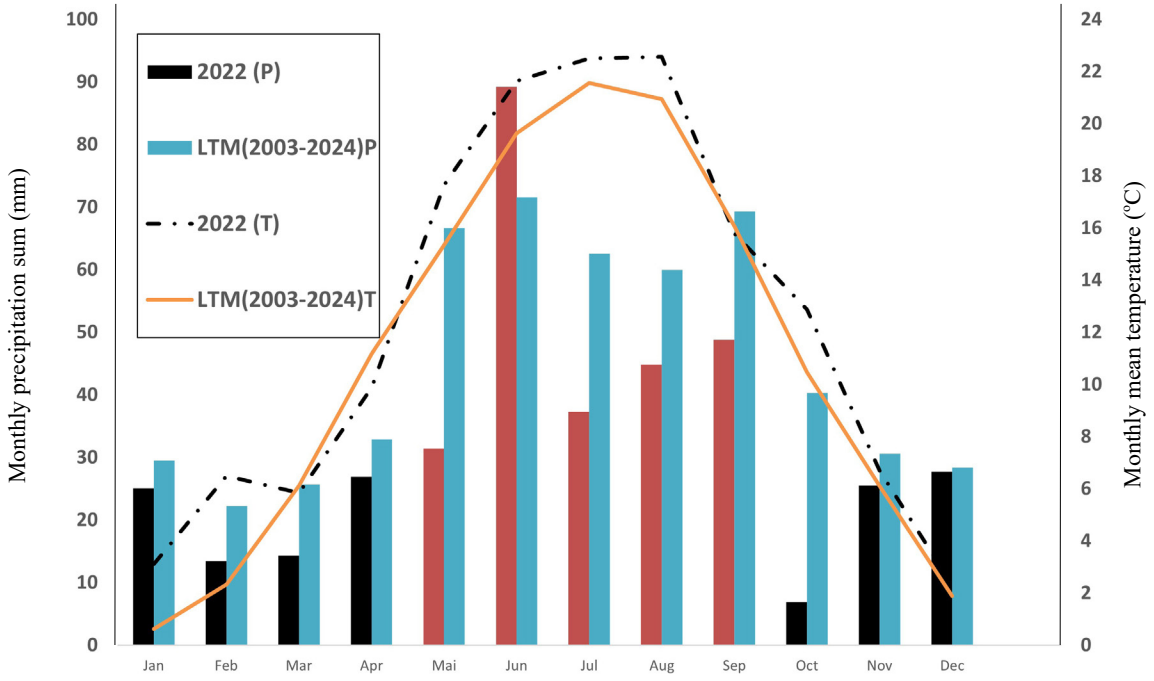

Fig. 4. Monthly precipitation sums (2022) compared with the monthly mean annual temperatures (2022), highlighted (red) bar shows the precipitation of the assumed maize and soybean growing period and the monthly precipitation (MJJAS), orange line shows the LTM (long-term-mean) 2003-2024 in temperature, blue bars show the LTM 2003-2024 in precipitation, P – precipitation, T – temperature.

August 1 to August 3, 2022. This data gap was addressed by using records from the GEOSPHERE/ZAMG station in Groß-Enzersdorf.

2.6. Wind downscaling

For the comparison of the different measured *WV* at a height of 2 m, the values were downscaled from the reference stations (W10H-BFW; MAIZEREF) from the original measurement height of 10 to 2 m above ground level using Eq. (1), as proposed by Allen *et al.* (1998):

$$u2 = u10\frac{4.87}{ln\,(67.8\ \times 10 - 5.42)}, \tag{1}$$

where: $u2$ – wind velocity at 2 m above ground level (m s^{-1}), $u10$ – wind velocity at 10 m above ground level.

2.7. Hedgerow coefficient

We used a simple scaling coefficient (Eq. (2)) as an indicator that can allow spatial extrapolation of the wind reduction effect (*WRE*) of landscape elements. The hedgerow coefficient (Δf) includes the wind barrier height (*hb*) and the distance to the barrier (*db*) in the calculation. In addition, the mean daily wind reduction *WRE* was included in the calculation. The WRE was calculated based on the mean daily *WV* at the observed plots with a hedgerow of deciduous shrubs and trees as well as a maize canopy as windbreaks. The *WRE* was referenced to the *WV* of the weather stations out of the windbreak distance on both investigated sites.

$$\Delta f = \frac{\left(\frac{hb}{db}\right)}{WRE}, \tag{2}$$

where: Δf – hedgerow coefficient, *hb* – height of the barrier (m), *db* – distance to the barrier (m), *WRE* – mean daily wind reduction at *db* (m s^{-1}).

The aim of the calculation is to find out the wind-reduction effect of the investigated WPS (crop canopy-based and deciduous hedgerow-based). By using this indicator, upscaling from point-based measurement to a larger spatial scale is possible, as are comparisons with other WPS types once they are parameterized for different types of WPSs.

2.8. Evapotranspiration model

2.8.1. Grass reference evapotranspiration (Et_0)

The FAO Penman-Monteith method adapted by Allen *et al.* (1998) is maintained as the sole standard method for the computation of Et_0 and Et_a from meteorological data. This method was used to capture wind-dependent evapotranspiration at the WPS and SICE sites (Eqs (3) and (4)). For our purpose, the calculation was done with the help of an Excel calculation sheet, where daily meteorological data derived from the field experiment measurements were used as input (*WV*, A*T, RH, GR, P*). The grass reference evapotranspiration (Et_0) was calculated as:

$$Et_0 = \frac{0.408\Delta\,(GR - G) + }{\Delta + \gamma\,(1 + 0.34WV)}$$
$$+\frac{\gamma\frac{900}{AT+273}WV\,(es - ea)}{\Delta + \gamma\,(1 + 0.34WV)}, \quad (3)$$

where: Et_0 – grass reference evapotranspiration (mm day^{-1}), GR – net radiation at the crop surface (MJ m^{-2} day^{-1}), G – soil heat flux density (MJ m^{-2} day^{-1}), AT – air temperature at 2-m height (°C), WV – wind velocity at 2-m height (m s^{-1}); es – saturation vapor pressure, ea – actual vapor pressure, es-ea – saturation vapor deficit (kPa); Δ – slope vapor pressure curve, Υ – psychrometric constant (kPa °C^{-1}).

2.9. Actual evapotranspiration (Et_a)

To calculate the actual evapotranspiration (Et_a), the crop factor (kc) development over the growing season was estimated from the observed development of plant height and the leaf area index, whereas the factor ks was estimated by considering the effect of soil water depletion on Et_a using a linear approach (Allen *et al.*, 1998). Both factors (ks, kc) are empirical and showed the best congruence with measurements in daily resolution. The evapotranspiration (Et_a) was calculated as:

$$Et_a = Et_0\,kc\,ks, \quad (4)$$

where: Et_a – actual evapotranspiration (mm day^{-1}), kc – crop factor (0.1-1.2), ks – soil water depletion factor (0-1).

3. RESULTS

3.1. Wind velocities at the WPS and SICE sites

We compared WV at multiple distances from the hedgerow of 10 times the height (10H, H = 10 m) on both leeward (L10H) and windward sides (W10H), as well as at 2H, 4H, and 6H leeward (L2H, L4H, L6H) (Fig. 1a-b). The WRE was most pronounced at L2H for both measurement heights (1 and 2 m above ground level (a.g.l.)), whereas the WRE decreased progressively at L4H and L6H. Replication plots (*e.g.*, L2H-BFW *vs*. L2H-BOK) showed consistent patterns.

The WRE was strongest at the closest leeward plots (L2H-BOK, L2H-BFW). At L6H-BOK, WV data were incomplete due to sensor failure from June 8, 2022, and onward, so gap-filling was performed with the help of the replication plot (L6H-BFW). Table 1 summarizes the mean WV and statistical metrics for all plots. The highest values occurred at L10H-BOK (2.0-2.5 m s^{-1}) and W10H-BFW (1.8-2.2 m s^{-1}), as shown in Fig. 5.

Figure 7 compares WV for the reference plots (PEAREF, MAIZEREF) and the SICE configurations. Two setups were analyzed: A (0.5H, 1H, 2H) and B (1H, 2H, 2.5H), which were measured at both measurement heights (1 and 2 m a.g.l). The results were compared to the reference stations and the SICE rows within the experimental area. A clear WRE was visible at both heights. Summary statistics (range, mean, standard deviation) for all plots are provided in Table 3.

3.2. Wind directions at the WPS and SICE sites

Figure 6a-e illustrate the distribution of WV across four wind sectors (WS) on the WPS plot (E-S-W-N; 0-90, 91-180, 181-270, and 271-360°) for each plot at two measurement heights (1 and 2 m a.g.l.). These sectors correspond to the main WDs (N, E, S, W) and allow analysis of WV patterns relative to the prevailing WD. WDs were normalized for comparison (to project a perpendicular WV onto the WPS) (Table 2). Dominant sectors varied among the plots: L2H-BOK was primarily influenced by sectors N and S, L4H-BOK was influenced by sector S, L6H-BOK was influenced by sectors E and S, L10H-BOK was influenced by sector N, L2H-BFW was influenced by sector N, L6H-BFW was influenced by sector N, and W10H-BFW was influenced by sectors N and W (Table 2). Fig. 8 present the WV distribution across WS for the SICE plots at both

Table 1. Overview of the wind velocities for each plot on the WPS site, observed period from DOY 95-184 in 2022, n = 13 084, based on daily mean values, – no data

Plot	Range (m s^{-1})			Mean (m s^{-1})		
	1 m	2 m	10 m	1 m	2 m	10 m
L2H-BOK	0.4-4.0	0.5-4.8	–	1.2 ± 0.7	1.4 ± 0.9	–
L4H-BOK	0.4-3.8	0.6-4.8	–	1.4 ± 0.9	1.6 ± 1.0	–
L6H-BOK	0.9-4.4	0.9-4.9	–	2.0 ± 0.9	2.1 ± 1.0	–
L10H-BOK	0.6-4.8	0.9-6.5	–	2.0 ± 0.9	2.5 ± 1.1	–
L2H-BFW	0.3-4.3	–	–	1.1 ± 0.8	–	–
L4H-BFW	–	–	–	–	–	–
L6H-BFW	0.6-4.0	–	–	1.6 ± 0.7	–	–
W10H-BFW*	0.6-5.5	0.8-5.3	1.1-7.1	1.8 ± 0.7	2.2 ± 0.9	2.9 ± 1.2

*Downscaled WV to 2 m measuring height.

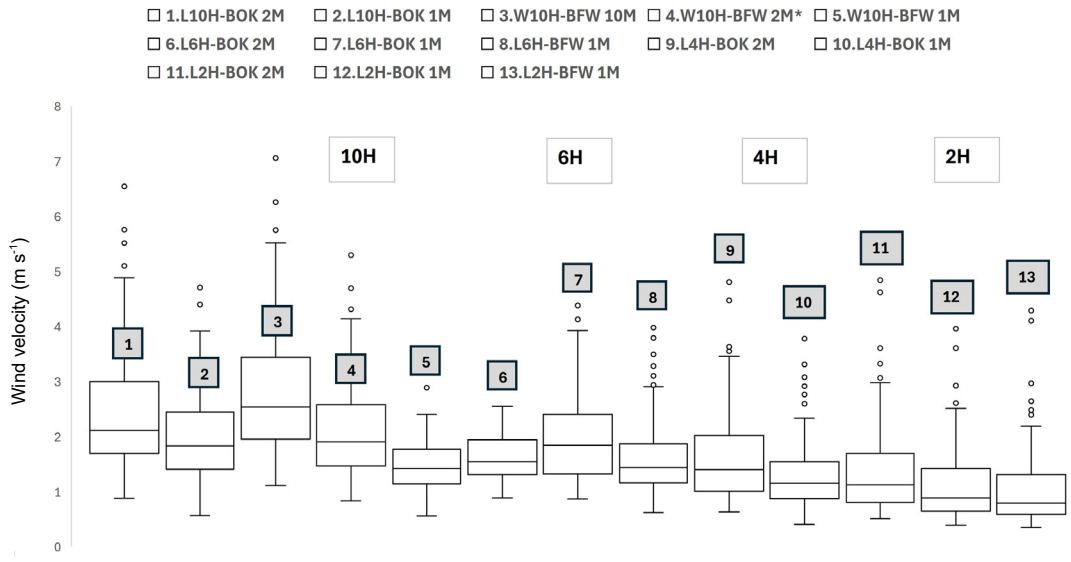

Fig. 5. Daily mean wind velocities from different plots on the WPS site in dependence to the distance to the hedgerow in respect to the hedgerow multiple height; black points are statistical outliers; 1 and 2 m define the measuring height of the wind sensors (a.g.l.), including of W10H-BFW 10M with 10 m measuring height (a.g.l.); *downscaled wind velocities data (plot W10H-BFW 2M); observed period from DOY 95-184; n = 13 084, based on daily mean values; for 2022.

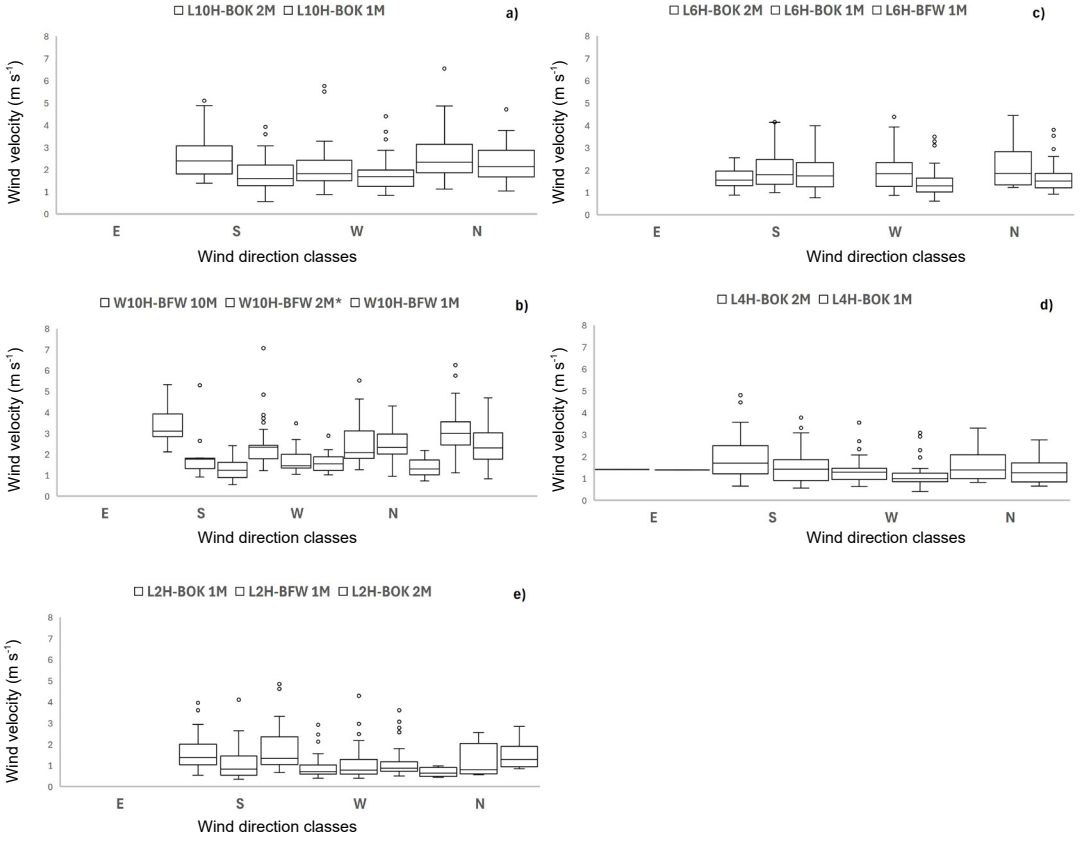

Fig. 6. Comparison of the daily mean wind velocities on the WPS plot in different measuring heights of each observed transect over the whole measurement period 2022 in combination with t,he different wind sectors: a) wind velocities on the plot (L10H-BOK 2 and 1 m measurement height (a.g.l.); b) wind velocities on the plot (W10H-BFW), 10 m, 2 m, 2 m* measurement height (a.g.l.),*downscaled wind velocity; c) wind velocities on the plot (L6H-BOK, L6-BFW) in 2 m and measurement height (a.g.l.); d) wind velocities on the plot (L4H-BOK) 2 m and 1 m measurement height (a.g.l.); e) wind velocities on the plot (L2H-BOK; L2H-BFW) 2 and 1 m measurement height (a.g.l.), the wind directions are divided into 4 sectors. Sector 1 (0-90°), sector 2 (91-180°), sector 3 (181-270°), sector 4 (271-360°). The sectors correspond to the main geographic directions. (DOY 85-184); n = 13 084; dots without fillings are outliers.

Table 2. Overview of the wind directions on the WPS site; observed period from DOY 95-184; n = 13 084, based on daily mean values; for 2022; letters (N-E-S-W) representing the wind sectors (E-S-W-N, 0-90°, 91-180°, 181-270°, 271-360°), corresponding to the main geographic directions

Plot	Measurement height*	
	2 m	1 m
L2H-BOK	W > S > E > N	E > S > W > N
L4H-BOK	E > W > S > N	E > W > S > N
L6H-BOK	N	E > S > W > N
L10H-BOK	W > E > S > N	W > E > S > N
L2H-BFW	n.a.	W > S > E > N
L6H-BFW	n.a.	W > S > E > N
W10H-BFW*	W > S > N > E	S > E > W > N

*Downscaled *WV* to 2 m measuring height.

heights. The *WV*s at the reference station were highest in the following order: E > S > N > W. In setup A, the order of sector dominance was N > W > S > E, while in setup B, it shifted to E > N > W > S.

3.3. Wind reduction effect at the WPS and SICE sites

The WPS substantially reduced *WV*, and the strongest WRE was observed at the closest leeward plots (Table 4). The WRE decreased with the increasing distance from the barrier, as expected. The SICE also demonstrated a significant WRE, which was most pronounced at the 2-m measurement height (Table 5).

3.4. Hedgerow coefficient (Δ*f*) for comparing the WPS and SICE plots

Figures 9 and 10 illustrate the relationship between barrier height and *WV* reduction for both systems. The coefficient Δ*f* was calculated according to Eq. (2). As anticipated, the *WRE* declined with the distance from the barrier. Differences between the dominant *WS* and measurement heights influenced the observed patterns, with

Table 3. Overview of the wind velocities for each plot on the SICE site (PEAREF, MAIZEREF), 1. setup: A0.5H; A1H; A2H, 2. setup: B1H; B2H; B2.5H; n =17 133, based on daily mean values; for 2022, observed period from 1. setup: DOY 186-208; 2. setup: DOY 209-304

Plot	Range (m s^{-1})				
	1 m	2 m	10 m*	1 m	2 m
PEAREF	0.2-3.1	0.3-4.7	–	0.7 ± 0.5	1.5 ± 0.9
MAIZEREF	x	0.5-4.1	0.7-5.5	–	1.6 ± 0.8
1. SETUP A0.5H	0.3-0.9	0.4-1.7	–	0.2 ± 0.2	0.3 ± 0.3
1. SETUP A1H	0.3-1.0	0.4-2.1	–	0.6 ± 0.2	1.1 ± 0.4
1. SETUP A2H	–	–	–	–	–
2. SETUP B1H	0.5-4.0	0.4-3.5	–	0.9 ± 0.7	1.3 ± 0.6
2. SETUP B2H	0.4-4.5	0.3-3.7	–	0.8 ± 0.8	1.4 ± 0.6
2. SETUP B2.5H	0.2-3.1	0.5-3.8	–	0.7 ± 0.6	1.4 ± 0.8

*Downscaled *WV* from 10 m to 2 m, W*V* in MAIZEREF was logged in 10 m measurement height, additional information: sensor on plot 1.setup A2H was for the observed period down (no datasets), – missing values.

Table 4. Mean *WV* reduction (%) on the WPS site; *WV* W10H-BFW (1 m, 2 m MH) is compared with the *WV* on the plots (L10H-BOK, L6H-BOK, L4H-BOK, L2H-BOK and L2-BFW, L6-BFW) in the measurement heights 1 and 2 m a.g.l., based on the mean daily *WV*, DOY 186-304, n = 10 488

Reference wind velocity 1 m/ 2 m*				
L10H/ (1 m MH)	L10H/ (2 m MH)	L6H/ (1 m MH)	L6H/ (2 m MH)	L6H/ (1 m MH)*
1%	9%	34%	39%	11%
L4H/ (1 m MH)	L4H/ (2 m MH)	L2H/ (1 m MH)	L2H/ (2 m MH)	L2H/ (1 m MH)*
24%	30%	35%	40%	41%

*Upscaled *WV* in 2 m measurement height (a.g.l.) (W10H-BFW) was used.

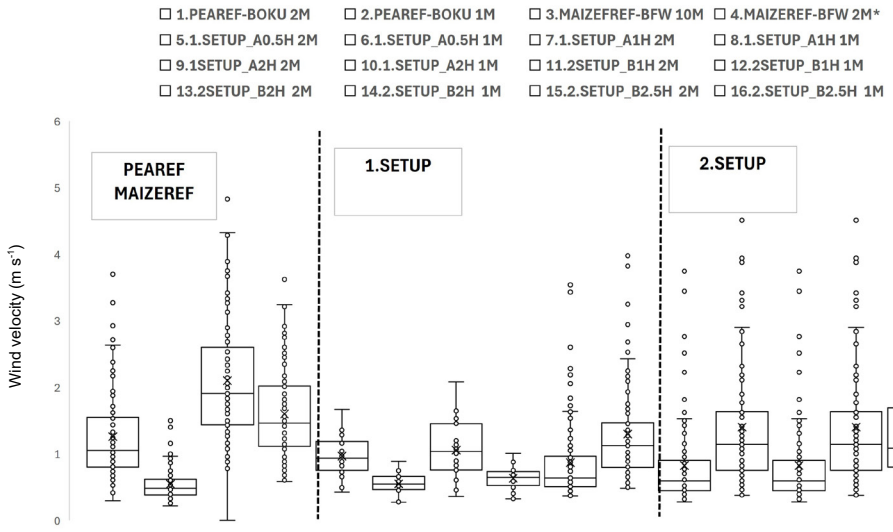

Fig. 7. Daily mean wind velocities on the SICE site in dependence to the distance of the multiple canopy height to the maize strip leewards (1. setup A0.5H; A1H, A2H; 2. setup B1H; B2H; B2.5H), black points are statistical outliers; 1 and 2 m define the measuring height of the wind sensors (a.g.l.), except of MAIZEREF-BFW with 10 m measuring height (a.g.l.); *downscaled wind velocities data (plot MAIZEREF-BFW-2M); observed period from DOY 186-208 (1. setup) and DOY 209-304 (2. setup); n =17 133; based on daily mean values for 2022.

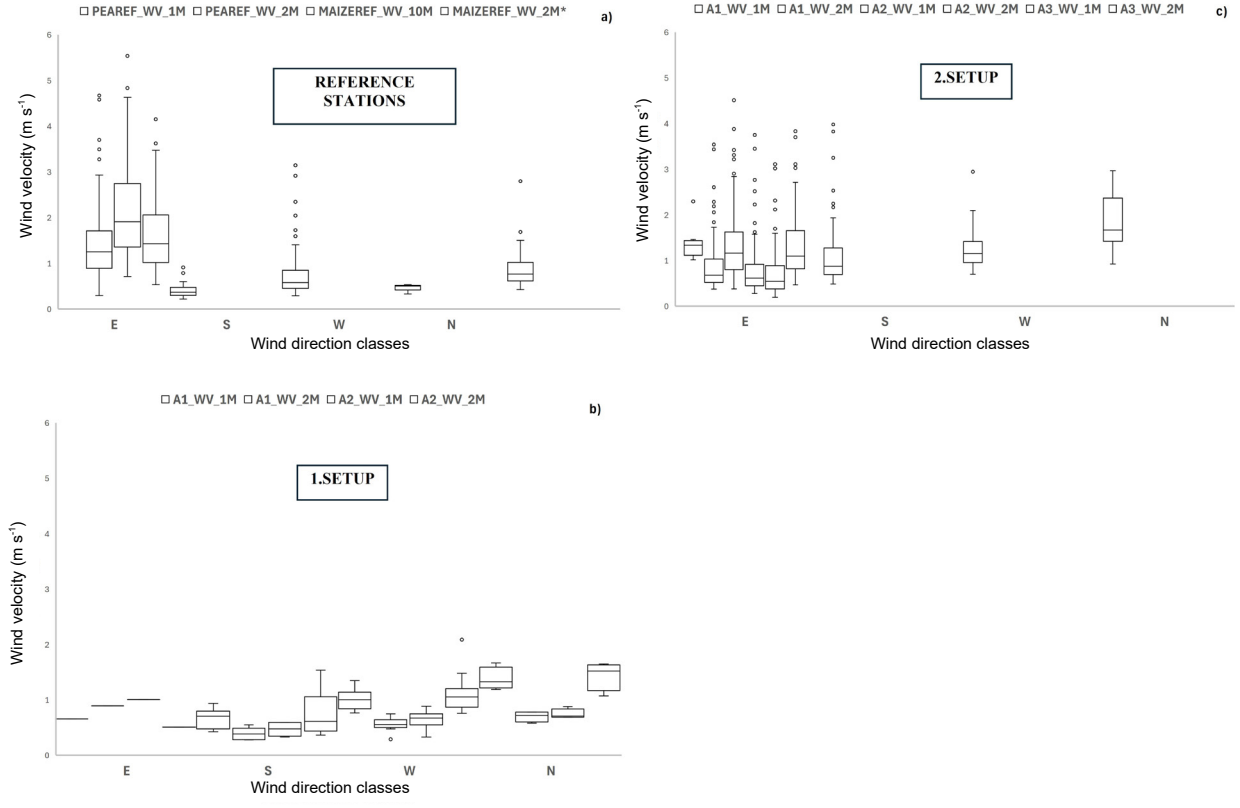

Fig. 8. Comparison of the daily mean wind velocities on the SICE site in different measuring heights of each observed transect over the whole measurement period 2022 in combination with the different wind sectors: a) wind velocities on the plot (PEAREF; MAIZEREF) 2 m, 2 m*, 1 m and 10 m measurement height (a.g.l.),*downscaled wind velocity; b) wind velocities on the plot (1. setup A0.5H-A2H,) 1 and 2 m measurement height (a.g.l.); c) wind velocities on the plot (2.setup B1H- B2.5H) in 1 and 2 m measurement height (a.g.l.); the wind directions are divided into 4 sectors. Sector 1 (0-90 g), sector 2 (91-180 g), sector 3 (181-270 g), sector 4 (271-360 g). The sectors correspond to the main geographic directions (1. setup: DOY 186-208; 2. setup: DOY 209-304); n =16 814 (PEAREF, MAIZEREF), n = 3 313 (1. setup), n = 13 681 (2. setup), based on daily mean values; for; dots without fillings are outliers.

Table 5. Mean *WV* reduction in % on the SICE site; *WV* MAIZEREF (1 m, 2 m MH) and *WV* PEAREF (1 m, 2 m MH) is compared with the *WV* on the plots (1. setup A0.5H- A2H and 2. setup B1H- B2.5H); on the plot A0.5H and A2H no comparison was done (missing data), based on the mean daily *WV*; DOY 186-304, n = 13 566

	Reference wind velocity					
1. SETUP MAIZEREF MH 10 m	A0.5H (1 m MH)	A0.5H (2 m MH)	A1H (1 m MH)	A1H (2 m MH)	A2H (1 m MH)	A2H (2 m MH)
MH 2 m*	–	31%	–	23%	–	–
2. SETUP PEAREF MH 1 m	B1H (1 m MH)	B1H (2 m MH)	B2H (1 m MH)	B2H (2 m MH)	B2.5H (1 m MH)	B2.5H (2 m MH)
MH 2 m	0%	42%	3%	46%	36%	56%

Table 6. Overview of the calculated daily grass reference evapotranspiration (Et_0) rates WPS site in 2 m measurement height (a.g.l.) (W2H-BFW, W10H-BFW, L2H-BFW, L4H-BFW, L6H-BFW, L2H_BOK, L4H-BOK, L6H-BOK, L10H-BOK), observed period from DOY 95-159 in 2022

Plot	L2H-BOK	L4H-BOK	L6H-BOK*	L10H-BOK	W10H-BFW*
Range	0.5-4.2	1.5-6.9	0.6-4.2	0.1-7.6	0.6-2.6
Mean	2.0 ± 0.8	3.6 ± 1.0	1.9 ± 0.8	3.7 ± 2.5	2.6 ± 1.0
Total sum	130	420	171	331	234
n	12 960	12 960	9 360	12 960	12 960

*Downscaled *WV*, all values mm d^{-1}.

Table 7. Overview of the calculated actual evapotranspiration (Et_a) rates 2022 – WPS (measuring height 2 m (a.g.l.) on the plots (L2H-BOK, L4H-BOK, L6H-BOK, L10H-BOK, L2H-BFW, L4H-BFW, L6H-BFW, W2H-BFW, W10H-BFW); observed period from DOY 95-184; *not complete dataset implemented

Plot	L2H-BOK	L4H-BOK	L6H-BOK*	L10H-BOK	W10H-BFW*
Range	1.3-5.9	0.1-6.2	0.4-5.9	0.1-5.7	0.1-7.2
Mean	2.0 ± 1.3	2.2 ± 1.3	1.9 ± 1.3	1.5 ± 1.3	1.5 ± 1.5
Total sum	177	198	124	177	177
n	12 960	12 960	9 360	12 960	12 960

*Downscaled *WV*, all values mm d^{-1}.

SW-NW winds contributing most strongly at higher height-to-distance ratios, given the NE-SW row orientation. Overall, the ratio of barrier height to distance emerged as the key determinant of the *WRE* across both systems and provides a basis for extrapolating windbreak effects across agricultural landscapes.

3.4.1. Evapotranspiration rates (Et_0, Et_a) at the WPS site

The highest Et_0 rates were observed at the 10-fold hedgerow distance (L10H-BOK and W10H-BFW) except for L4H-BOK, where an unexpectedly high mean Et_0 (3.6 ± 1.0 mm day^{-1}) was recorded, which was also reflected in the cumulative Et_0 sum (Table 6). To further analyze the relationship between the wind reduction effect (*WRE*) and Et_0, daily evapotranspiration rates were compared with the prevailing *WS* for each plot (Fig. 11). At L10H-BOK (2 m a.g.l.), the ranking of Et_0 was WS, S > W > N > E, while at W10H-BFW, the order was N > S > W > E, and at L6H-BOK, it was S > N > W > E. These patterns closely correspond to the respective WRE trends (Fig. 11a-f). Statistical summaries are presented in Table 6.

Et_a was derived from Et_0 estimates (Eq. (4)), and the results are summarized in Table 7 and visualized by *WS* in Fig. 12. For 2022, the dominant *WS*s for Et_a at L10H-BOK, W10H-BFW, and L6H-BOK were S > N > W > E. At L4H-BOK, the same order was observed (S > N > W > E), while L2H-BOK's ranking was S > W > N > E. At L6H-BFW, WS E dominated (E > N > W > S). The cumulative

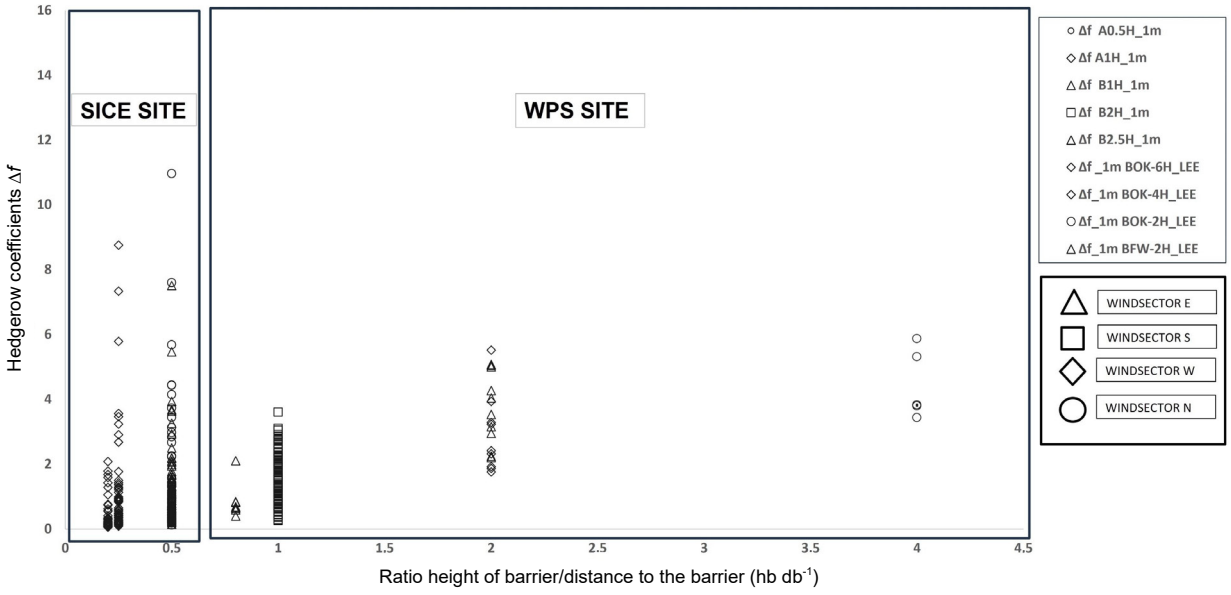

Fig. 9. Comparison of the hedgerow coefficients in 1 m measuring height (a.g.l.) *vs*. height of the barrier/distance to the barrier, the most common wind direction were shown by symbols, DOY 95-184, n = 12 816, calculation of hedgerow coefficients based on daily mean wind reductions.

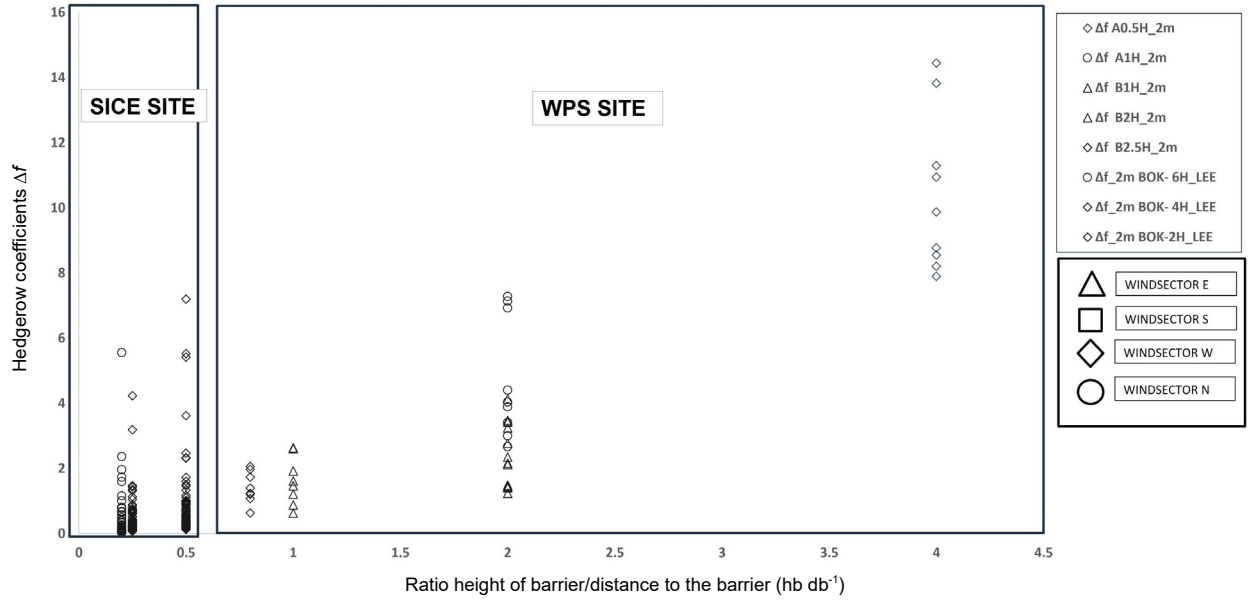

Fig. 10. Comparison of the hedgerow coefficients in 2 m measuring height (a.g.l.) *vs*. height of the barrier/ distance to the barrier, the most common wind direction were shown by symbols, DOY 95-184, n = 12 816, calculation of hedgerow coefficients based on daily mean wind reductions.

Et_a within the observed period ranged from 198 to 177 mm as the total sum across plots, with differences reflecting the distance to the windbreak. Only one plot (incomplete dataset) showed a markedly lower total (124 mm). Overall, Et_a reductions relative to Et_0 indicated a measurable influence of the WRE.

3.4.2. Evapotranspiration rates (Et_0, Et_a) at the SICE site

Et_0 was calculated for reference plots (PEAREF, MAIZEREF) and two experimental setups: setup 1 (A0.5H-A2H) and setup 2 (B1H-B2.5H) at two heights (1 and 2 m a.g.l.). Statistical summaries are provided in Table 8. In setup 1, the mean Et_0 rates were higher than at the reference plots, although cumulative Et_0 sums remained similar. In setup 2, the mean and cumulative Et_0 values closely matched the reference plots (Table 8). WS analysis at 2 m revealed consistent patterns: at PEAREF and MAIZEREF, the Et_0 ranking was E > S > W > N. In setup 1 (A0.5H, A1H), the order was reversed (N > W > S > E), whereas in setup 2 (B1H, B2H, B2.5H), the sequence followed the reference plots (E > S > W > N) (Fig. 13).

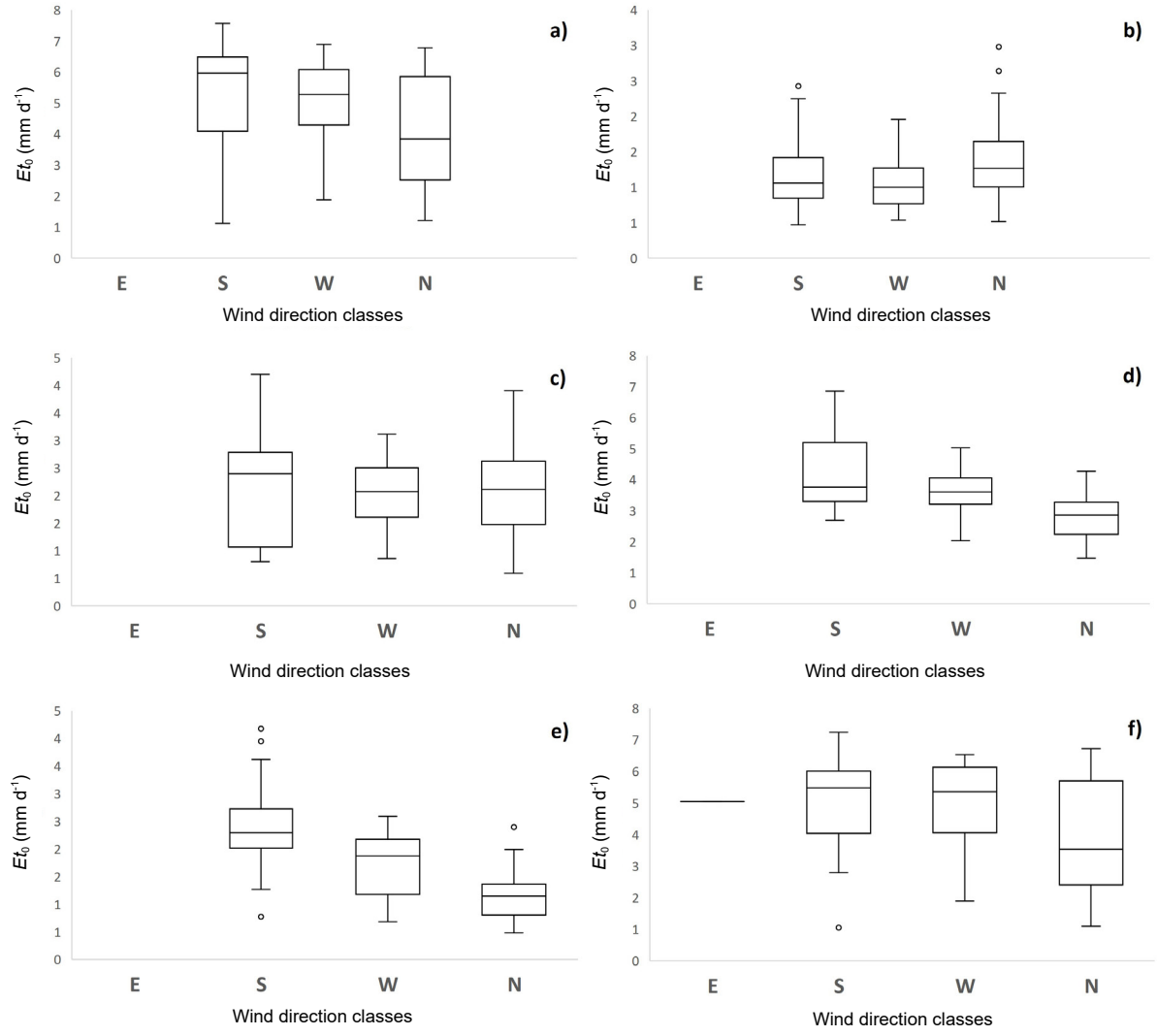

Fig. 11. Comparison of the daily grass reference evapotranspiration (Et_0) rates, (calculated FAO Allen *et al*. (1998) approach) 2022 of each observed plots (L10H-BOK-L6H-BOK; W10H-BFW, L6H-BFW) on the WPS site in connection with 4 main wind sectors based on the daily mean wind directions and the daily mean wind direction over the whole measurement period (DOY 95-184); n= 13 680; all values in 2 m MH (a.g.l.): a) evaporation rates on the L10H-BOK; b) evaporation rates on the W10H-BFW plot; c) evaporation rates on the L6H-BOK plot; d) evaporation rates on the L4H-BOK plot; e) evaporation rates on the L2H-BOK plot; f) evaporation rates on the L6H-BFW. The wind directions are divided into 4 sectors. Sector 1 (0-90 g), sector 2 (91-180 g), sector 3 (181-270 g), sector 4 (271-360 g). The sectors correspond to the main geographic directions.

*WS*s with the highest *WV* corresponded to those with the highest Et_0 rates, indicating a direct link between wind exposure and evapotranspiration. Et_a was derived from Et_0 calculations (Eq. (4)), and statistical results are summarized in Table 9, while *WS*-related distributions are shown in Fig. 14a-c. In 2022, *WS* E dominated Et_a at PEAREF and MAIZEREF. In setup 1, plots A0.5H and A1H showed an Et_a ranking of S > W > N > E, while the data from A2H were insufficient. In setup 2, WS E dominated all plots (B1H, B2H, B2.5H) at 2 m. The cumulative Et_a was lower than Et_0 for both reference and experimental plots, reflecting the WRE, which was caused by the barrier influence (Fig. 14). The reduction magnitude varied with the distance from the wind barrier, which highlights the influence of local microclimatic conditions on the actual evapotranspiration (Table 9).

4. DISCUSSION

This case study analyzed two different wind protection systems (WPS and SICE). In-situ micro-meteorological transect measurements were conducted in 2022 at two close sites: a hedgerow-based WPS, where four measurement transects (windward and leeward of the windbreak in relation to the main wind direction) were examined, and

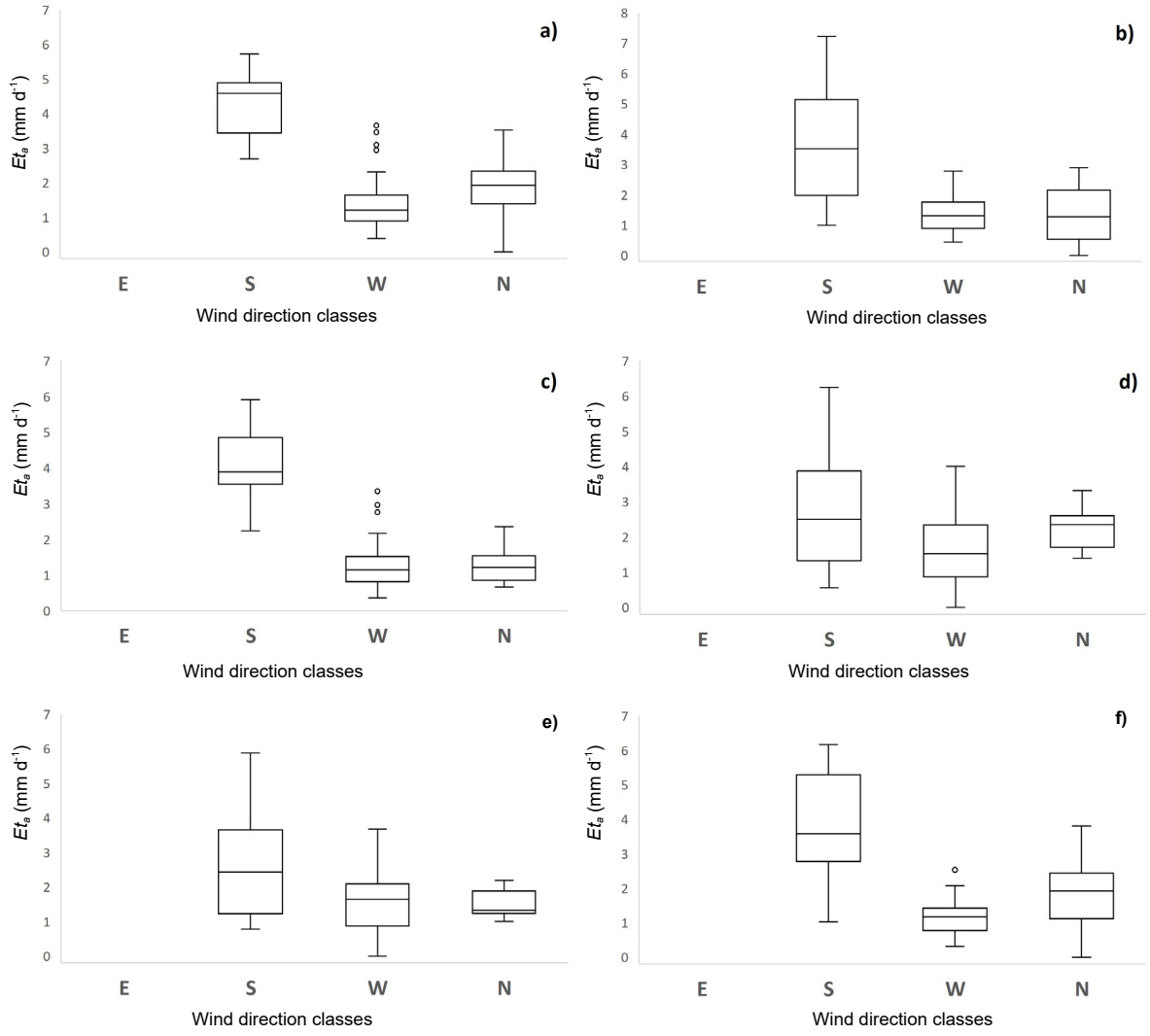

Fig. 12. Comparison of the actual evapotranspiration (Et_a) rates (calculated FAO approach) 2022 of each observed plots (L10H-BOK-L6H-BOK; W10H-BFW) on the WPS plot in connection with 4 main wind sectors based on the daily mean wind directions and the daily mean wind direction over the whole measurement period (DOY 95-184); n = 13 680, all values in 2 m MH (a.g.l.): a) evaporation rates on the L10H-BOK plot; b) evaporation rates on the W10H-BFW plot; c) evaporation rates on the L6H-BOK plot; d) evaporation rates on the L4H-BOK plot; e) evaporation rates on the L2H-BOK plot; f) evaporation rates on the L6H-BFW plot.

Table 8. Overview of the calculated (Et_0) rates on the SICE site in 2 m measurement height (a.g.l.) (MAIZEREF, PEAREF, 1. setup A0.5H- A2H, 2. setup B1H- B2.5H) and the modelled evaporation rates for comparison, observed period from DOY 186-208 (1. setup) and DOY 210-304 (2. setup) in 2022

Plot	MAIZEREF**	PEAREF	1. Setup			2. Setup		
			A0.5H	A1H	A2H	B1H*	B2H	B2.5H*
Range	0.3-6.7	0.3-6.3	1.7-6.2	1.7-6.2	-	1.5-5.8	1.5-5.8	2.9-5.6
Mean	3.1 ± 1.7	3.0 ± 1.6	4.7 ± 1.5	4.7 ± 1.4	-	4.0 ± 1.2	4.0 ± 1.2	3.8 ± 1.1
Total sum	370	357	108	109	-	232	234	225
n	13 566	13 566	2 622	2 622	0	10 488	10 488	10 146

*Not complete dataset implemented; **downscaled *WV*.

Table 9. Overview of the calculated actual evapotranspiration (Et_a) rates 2022 on the SICE site (MAIZEREF, PEAREF, 1. setup A1-A3, 2. setup A1-A3); observed period from DOY 186-208 (1. setup) and DOY 210-304 (2.setup), measuring height 2 m (a.g.l.)

Plot	MAIZEREF**	PEAREF	1. Setup			2. Setup		
			A0.5H	A1H	A2H	B1H*	B2H	B2.5H*
Range	0.1-9.0	0.1-8.3	0.4-8.4	0.4-8.5	–	0.2-8.0	0.2-8.0	0.1-7.7
Mean	2.3 ± 1.7	2.3 ± 1.6	3.9 ± 1.5	3.9 ± 1.4	–	2.3 ± 1.2	2.3 ±1.2	2.3 ± 1.1
Total sum	278	270	89	89	–	221	222	219
n	13566	13566	2622	2622	0	10488	10488	10146

*Not complete dataset implemented, **downscaled *WV*.

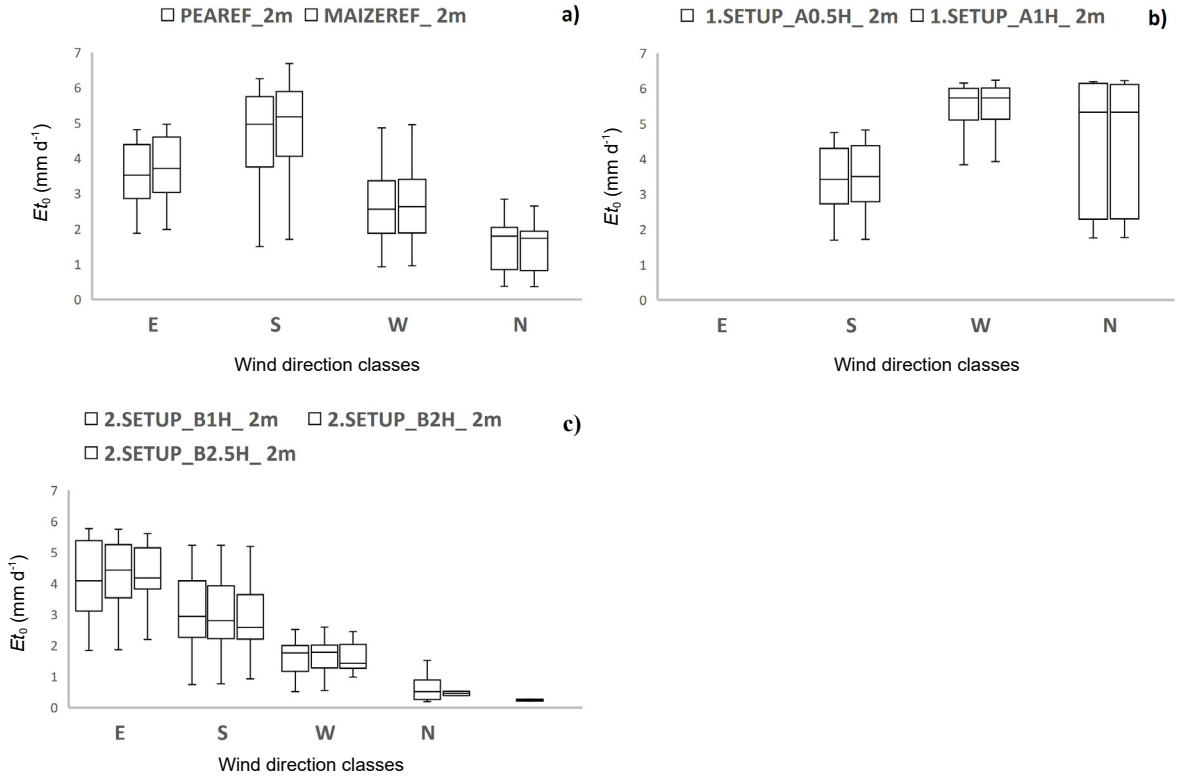

Fig. 13. Comparison of the actual evapotranspiration rates (Et_0, calculated FAO approach) 2022 of each observed plots (MAIZEREF, PEAREF, 1.setup A0.5H-A2H, 2. setup B1H-B2.5H) on the SICE site in connection with 4 main wind sectors based on the daily mean wind directions and the daily mean wind direction over the whole measurement period (1. setup: DOY 186-208, 2. setup: DOY 210-304); n = 18814: a) Et_0 rates on the PEAREF and the MAIZEREF plot in 2 m measurement height (a.g.l.), 2 m data was downscaled from 10 m measurement height; b) Et_0 rates on the 1. setup A0.5H-A2H plot in 2 m measurement height (a.g.l.), A2H data is missing in both measurement heights; c) Et_0 on the 2. setup B1H-B2.5H plot in 2 m measurement height (a.g.l.).

a crop-based system (SICE) with maize and soybean, where the maize strips were used as a windbreak. Field observations and measurements were carried out over a six-month period during the growing season, and microclimatic measurements were taken.

The measured microclimatic parameters included *WV*, *AT*, *RH*, and *GR*. Based on the measured meteorological variables, the grass reference evapotranspiration (Et_0) and crop-specific actual evapotranspiration (Et_a) rates were simulated and analyzed in the context of four primary *WD*s. At the WPS site, the *WV* peaks and mean *WV* values decreased in the immediate vicinity of the windbreak and increased with the distance from it. This effect was observed at both measurement heights of 1 and 2 m.

These findings align with data from similar experiments (He *et al.*, 2017; Böhm *et al.*, 2014; Dufkova, 2007; Peri *et al.*, 2002). Wind reductions from these studies indicated WREs at about 85% (Peri), 78% (Dufkova), and 50% (Böhm), which depended on the distance to the wind barrier. The results from our study were within this range (*e.g.*, 1-41% for the WPS system and 3-56% for the SICE).

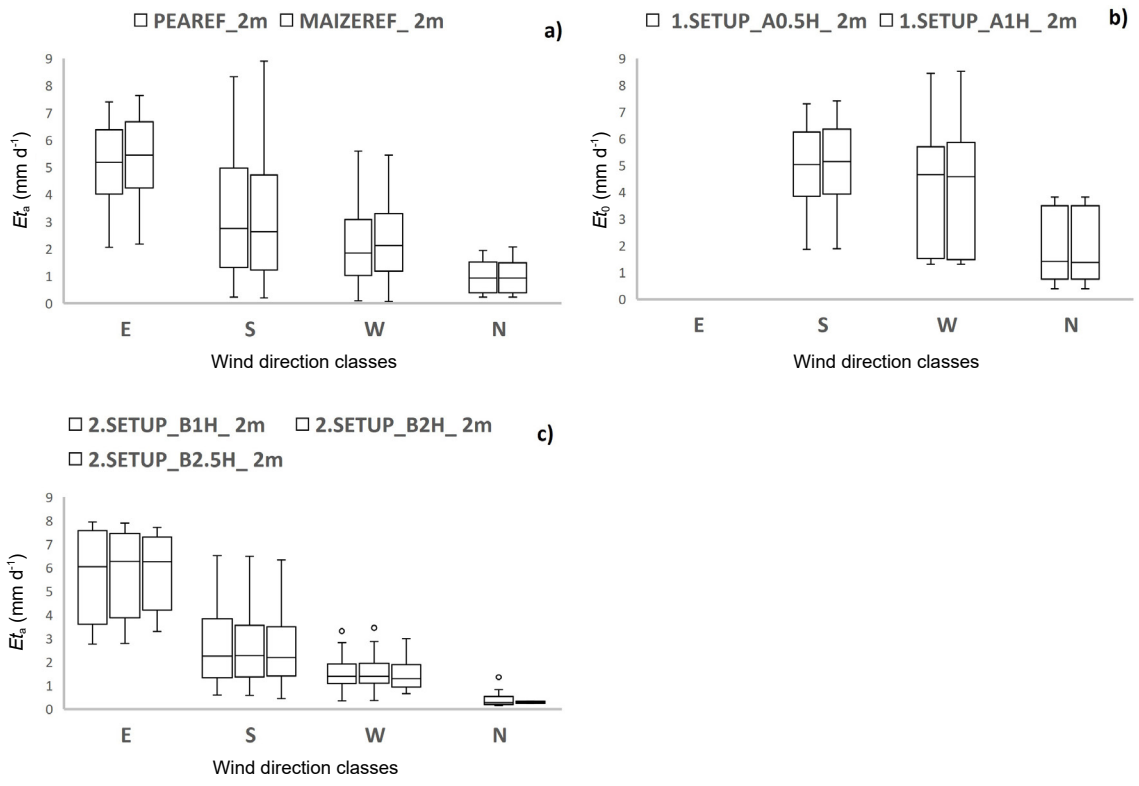

Fig. 14. Comparison of the actual evapotranspiration rates (Et_a, calculated FAO Allen *et al*. (1998) approach) 2022 of each observed plots (MAIZEREF, PEAREF, 1. setup A0.5H- A2H, 2. setup B1H-B2.5H) on the SICE plot in connection with 4 main wind sectors based on the daily mean wind directions and the daily mean wind direction over the whole measurement period (1. setup: DOY 186-208, 2. setup: DOY 210-304); n = 18814: a) Et_a rates on the PEAREF and the MAIZEREF plot in 2 and 1 m measurement height (a.g.l.), 2 m data was downscaled from 10 m measurement height; b) Et_a rates on the 1. Setup, A0.5H- A2H plot in 2 m and 1m measurement height (a.g.l.), A2H data is missing in both measurement heights; c) Et_a on the 2. Setup, B1H- B2.5H plot in 2 m and 1m measurement height (a.g.l.).

Table 10. Overview of the observed plots on the *WPS* site and the measured microclimatic parameters for both transects (Lee and Windwards)

Plot/Station	Measurement height (m a.g.l.)	Measurement depth (cm b.m.l.)	Measured parameter	Sensor type
BFW (Luv)	2/1		air temperature	ATMOS 41
L2H-BFW)	2		relative air humidity	ATMOS 41
L6H-BFW			wind direction	ATMOS 22
W2H-BFW	2/1		wind velocity	ATMOS 22
W10H-BFW	10		soil moisture	ATMOS 22
		15/30	soil temperature	TEROS 11/TM-4
		15/30	global radiation	TEROS 11/TM-4
	2		air temperature	ATMOS 41
BOKU (Lee)	2/1		relative air humidity	ATMOS 41
L2H-BOKU	2		wind direction	ATMOS 41
L4H-BOKU			wind velocity	ATMOS 22
L6H-BOKU	2 / 1		global radiation	ATMOS 22
L10H-BOKU	2 / 1			ATMOS 22
	2			ATMOS 41

Table 11. Company names of the used data logger, type of the data loggers, logging interval and sampling interval for each observed location on the WPS site; *Campbell CR 10X on the A1-A3 plot was connected with the atmometers

Plot	Company	Type	Logging intervall	Sampling intervall	Station
BFW (Luv)	METER©, Pullman, USA	ZL6	10 min	1 min	L2H-BFW L6H-BFW W2H-BFW W10H-BFW
BOKU (Lee)	METER©, Pullman, USA	ZL6	10 min	10 min	L2H-BOK L10H-BOK
BOKU (Lee)	METER©, Pullman, USA	EM50	10 min	10 min	L4H-BOK L6H-BOK
BOKU (Lee)	ETGAGE©, Loveland, USA	atmometer	60 min	1 s	L2H-BOK L4H-BOK L6H-BOK
BOKU (Lee)	CAMPBELL SCIENTIFIC©, Logan, USA	data logger*	60 min	1 s	L2H-BOK L4H-BOK L6H-BOK

The SICE system was designed to assess the impact of varying strip widths of two crop types (maize and soybeans) of different growing height on microclimatic conditions, which is similar to reports by Ouda *et al.* (2007) and Blessing *et al.* (2022). A notable *WV* reduction was observed within the 6-m-wide soybean strip due to the presence of an adjacent maize strip with 2-m canopy height. The measured parameters were compared across the plots, including the mean *WV*, *WRE*, Et_0, and Et_a rates.

At the WPS plot, the mean *WV* of the reference plot W10H-BFW (2-m measurement height) on the windward (LUV) side of the WPS was 2.2 m s^{-1}, while on the leeward (LEE) side (L10H-BOK), the mean *WV* was 2.5 m s^{-1}. In comparison, the plot located closer to the WPS (L2H-BOK) had a lower *WV* of 1.4 m s^{-1}, corresponding to a reduction of 0.8-1.1 m s^{-1}, depending on the plot. At a 1-m measurement height, the *WV* reduction was 0.6-0.8 m s^{-1}. These results confirm a significant (and expected) wind-reducing effect of the WPS (Ableidinger *et al.*, 2020; Weninger *et al.*, 2022; Forman and Baudry, 1984). For example, in the studies by Ableidinger *et al.* (2020) and Forman and Baudry (1984), the WRE was up to 60% dependent on the distance to the wind barrier, and in the study by Weninger *et al.* (2022), a reduction in wind erosion of up to 30% was found.

A similar pattern was observed within the SICE, where *WV* reductions were recorded as follows: setup 1: A0.5H: 0.2 m s^{-1}, A1H: 0.6 m s^{-1}; setup 2: B1H: 0.9 m s^{-1}, B2H: 0.8 m s^{-1}, B2.5H: 1.4 m s^{-1}. This represents a *WV* reduction with a range of 0.2-1.3 m s^{-1}, depending on the distance to the WPS (maize barrier). At the WPS site, the *WRE* increased with the decreasing distance to the windbreak as well, with L4H-BOK showing a *WRE* of 24-30% at both measurement heights, while L2H-BOK showed a *WRE* of 35-40%. Other studies show similar results of 9.715% (Vacek *et al.*, 2018) and 60-80% (Ma *et al.*, 2019). Both studies also implemented the plant architecture as a wind barrier, which was not considered in our actual case study.

Concerning the SICE site, the *WRE* with respect to the reference in the first setup was 23-31% within subplots A0.5H-A2H. In the second setup, PEAREF was used as the reference, and the *WRE* values were as follows: B1H (0-42%), B2H (3-46%), and B2.5H (36-56%). In all cases, the WRE increased with the decreasing distance to the neighboring maize strip.

To describe the systematic *WRE* for the different windbreak types, a hedgerow coefficient (Δf) was established to standardize these effects for use in potential upscaling studies for various windbreaks over the landscape. The hedgerow coefficient is based on the *WRE*, which is related to the relationship of the height and distance to the wind barrier (tree hedge, maize strip). Additionally, the values were classified for the four *WD* sectors in the plot. The lowest hedgerow-coefficient values (high wind reduction effect) occurred in the immediate vicinity of the wind barrier, and the highest values (low effect) occurred with the increasing distance from the barrier with an almost linear relationship to the height of the barrier versus the distance-to-barrier coefficient. However, further evaluation and calibration of this method are recommended for considerable of certain hedgerow characteristics, such as the density.

The calculated Et_0 rates increased in accordance with the increasing *WV* with the increasing distance from the hedgerow WPS. At reference plots W10H-BFW and L10H-BOK, the mean Et_0 rates were 2.6 and 3.6 mm d^{-1}, respectively. Closer to the WPS (L2H-BOK and L6H-BOK), the Et_0 rates were lower (1.9-2.0 mm d^{-1}) except for L4H-BOK, which had an increased transpiration rate of 3.7 mm d^{-1}.

Table 12. Measured parameters on the observed plots on the SICE site (PEAREF, MAIZEREF) and the setup 1 and 2 (A0.5H-A2H; B1H-B2.5H) during the observed period, *below mineral horizon layer

Plot/Station	Measurement height (m a.g.l.)	Measurement depth (cm b.m.l)*	Measured parameters	Sensor type
1. setup:	2/1		air temperature	ATMOS 41
A0.5H(1 m)	2		relative air humidity	ATMOS 41
A1H(2 m)			wind direction	ATMOS 22
A2H(4 m)	2/1		wind velocity	ATMOS 22
	2/1		soil moisture	ATMOS 22
		5	soil temperature	TEROS 11/TM-4
		5		TEROS 11/TM-4
2. setup:			air temperature	
B1H(2 m)	2/1		relative air humidity	ATMOS 41
B2H(3.5 m)	2		wind direction	ATMOS 41
B2.5H(5 m)			wind velocity	ATMOS 22
	2/1		soil moisture	ATMOS 22
	2/1		soil temperature	ATMOS 22
	n/n	5		TEROS 11/TM-4
	n/n	5		TEROS 11/TM-4
PEAREF	2		air temperature	ATMOS 14
	2		relative air humidity	ATMOS 14
			precipitation	ATMOS 22
	2		global radiation	ATMOS 41
	2		wind direction	ATMOS 41
	2/1		wind velocity	ATMOS 22
	2/1		soil moisture	ATMOS 22
	n/n	0-12	soil temperature	TM-4
	n/n	0-12		TM-4
MAIZEREF	2		air temperature	ATMOS 14
	2		relative air humidity	ATMOS 14
			precipitation	ATMOS 22
	2		global radiation	ATMOS 41
	2		wind direction	ATMOS 41
	10		wind velocity	ATMOS 22
	10		soil moisture	ATMOS 22
	n/n	0-12	soil temperature	TM-4
	n/n	0-12		TM-4

The Et_a rates showed more variability as they are also related to water availability to soil crops. Therefore, using the same reference stations as for Et_0, the Et_a rates did not consistently decrease with the decreasing distance to the windbreak. This indicated that a decrease in evaporation losses leads to higher water availability to crops in the soil and keeps Et_a at a higher level near the windbreak due to water extraction by the roots from the deeper soil layers. This is confirmed by several studies showing increasing biomass production near windbreaks. For example, Kort (1988) showed a yield increase for corn (12%), barley (25%), and millet (44%) in the vicinity of WPS systems. Cleugh (1998) observed a yield increase of 7%.

Regarding the SICE (maize, soybean), the Et_0 rates at PEAREF and MAIZEREF were 3.0-3.1 mm d^{-1}, while the SICE plots (A0.5H-A2H) had consistently higher values averaging 4.7 mm d^{-1} at the 2-m measurement height. The evapotranspiration rates within the SICE were also higher in both setups (setup 1: 4.5-4.6 mm d^{-1}; setup 2: 3.7-4.0 mm d^{-1}). The Et_a rates at 2-m measuring height in both experiments were 2.3-3.9 mm d^{-1}, exceeding reference values.

Windbreaks and strip intercropping systems provide multiple benefits in wind-exposed agricultural areas, including improved microclimatic conditions, reduced evaporation losses, and reduced soil erosion, which lead to increased crop yields (Ableidinger *et al.*, 2020; Hanming *et al.*, 2012; Campi *et al.*, 2009). The orientation of the WPS or intercropping strips in relation to WD significantly influences microclimatic improvements (Brandle *et al.*, 2004; Blessing *et al.*, 2022). Studies suggest that the wind influence extends to a distance of up to 20 times the WPS's height. The wind influence was also measured at up to approximately 10 times the WPS height, and the strongest effects were observed on the leeward side of the windbreaks (Řeháček *et al.*, 2017).

Table 13. Company names of the used data logger, type of the data loggers, logging interval and sampling interval for each observed location (see Fig. 1), *Campbell CR 10X on the A0.5H-A2H plot was connected with an atmometer (data only for validation)

Plot	Company	Type	Logging intervall	Sampling intervall	Station
PEAREF	METER©, Pullman, USA	ZL6	10 min	1 min	PEAREF
MAIZEREF		ZL6		10 min	MAIZEREF
A0.5H-A2H		EM50		10 min	1.setup: A1(1 m) A2(2 m) A3(4 m) 2.Trial: A1(2 m) A2(3.5 m) A3(5 m)
A0.5H-A2H	ETGAGE©, Loveland, USA	atmometer	60 min	1 s	1.setup: A0.5H(1 m) A1H(2 m) A2H(4 m) 2.setup: B1H(2 m) B2H(3.5 m) B2.5H(5 m)
A0.5H-A2H	CAMPBELL SCIENTIFIC©, Logan, USA	data logger*	60 min	1 s	1.setup: A0.5H(1 m) A1H(2 m) A2H(4 m)´ 2.setup: B1H(2 m) B2H(3.5 m) B2.5H(5 m)

Within the SICE, the absolute *WD* effects were smaller than those observed near the WPS due to the lower height of the windbreak and were additionally affected by differing observation periods with different *WV*s. The Et_0 rates behaved as expected and increased with the distance from the maize strip except at 4 times the hedgerow distance, which was likely due to effects of wind turbulence (Kanzler *et al.*, 2018; Thevs *et al.*, 2017). However, the Et_a rates did not show a consistent trend, possibly due to turbulence effects on microclimatic parameters such as air temperature and air humidity. Finally, to describe the systematic effects of windbreak systems of different types, we introduced a hedgerow coefficient to compare different WPSs and SICEs with different architectures in a standardized way. This approach could be used for spatial upscaling of windbreak effects over larger areas of landscapes if a high-spatial-resolution map of landscape elements is available (*e.g.*, based on laser scans).

5. CONCLUSIONS

The results demonstrate that both hedgerow-based systems (WPS, deciduous type) and crop-based wind breaking systems (SICE, strip crop type) produce measurable reductions in *WV* in the range of 0.2-0.7 m s^{-1}, depending on the measurement height und distance to the WPS. The WPS achieved higher absolute wind reductions, whereas the SICE systems exhibited significant local effects immediately adjacent to the barriers. The calculated Et_0 and Et_a values highlight the influence of wind reduction on evapotranspiration, with total reductions in the range of 104-201 mm (WPS) and 189-262 mm (SICE), depending on the distance to the barrier.

The demonstrated hedgerow coefficient (Δf) could be used as a simple indicator for comparing different WPSs and allows extrapolation from point measurements to the landscape scale. Practically, this approach could inform land-use planning to optimize wind protection, minimize

soil-water losses, and mitigate crop-yield reductions in drought conditions. However, further research and measurement campaigns or related data sources are needed to extend the parameterization for different types of WPSs or hedgerows.

6. ACKNOWLEDGEMENTS

In general, I would like to dedicate this article to my father-in-law, Richard Retzl, who unfortunately passed away during the writing of this doctoral thesis. I would also like to thank Dr. habil. Kerstin Michel for her many suggestions, her quick answers to all my questions, and for always having an open ear for me in all scientific matters.

Conflict of interest: The authors declare there is no conflict of interest.

7. REFERENCES

Ableidinger, C., Erhart, E., Kromp, B., Hartl, W., 2018. Mehrnutzungshecken. Vielfältige Nutzung von Bodenschutzanlagen zur nachhaltigen Produktion, zur Erosionsvermeidung und zur Erhöhung der regionalen Wertschöpfung. Zwischenbericht BIO Forschung Austria.

Ableidinger, C., Erhart, E., Amadi, E., Schütz, C., Kromp, B., Hartl, W., 2020. Klimaschutz durch Bodenschutzanlagen. Endbericht Klimagrün (Interreg ACZ142). Eigenverlag Bio Forschung Austria, Wien. https://www.unserboden.at/files/1_endbericht_klimagr__n_forschungsstudie_bfa.pdf

Allen, R.G., Pereira, L.S., Raes, D., Smith, M., 1998. Crop evapotranspiration – Guidelines for computing crop water requirements. (F. -F. Nations, Hrsg.) FAO Irrigation Drainage Paper 56, Chapter 2.

Aust G., Pock H., Schild A., Horvath D., Amann C., Schaffer H., *et al.*, 2023. EBOD2. Acesssed on 24. 4. 2023 von EBOD2: https://bodenkarte.at

Böhm, C., Kanzler, M., Freese, D., 2014. Wind speed reductions as influenced by woody hedgerows grown for biomass in short rotation alley cropping systems in Germany. Agroforestry Systems 88, 579-591. https://doi.org/10.1007/s10457-014-9700-y

Bitog, J.P., Lee, I.B., Hwang, H.S., Shin, M.H., Hong, S.W., Seo, I.H., *et al.*, 2012. Numerical simulation study of a tree windbreak. Biosystems Eng. 111(1), 40-48. https://doi.org/10.1016/j.biosystemseng.2011.10.006

Blessing, D.J., Gu, Y., Cao, M., Cui, Y., Wang, X., Asante-Badu, B., 2022. Overview of the advantages and limitations of maize-soybean intercropping in sustainable agriculture and future prospects: A review. Chilean J. Agric. Res. 82(1), 177-188. http://dx.doi.org/10.4067/S0718-58392022000100177

Brandle, J.R., Hodges, L., Zhou, X.H., 2004. Windbreaks in North American agricultural systems. In New Vistas in Agroforestry: A Compendium for 1st World Congress of Agroforestry 65-78. Springer Netherlands. https://doi.org/10.1007/978-94-017-2424-1_5

Campi, P., Palumbo, A.D., Mastrorilli, M., 2009. Effects of tree windbreak on microclimate and wheat productivity in a Mediterranean environment. European J. Agronomy 30(3), 220-227. https://doi.org/10.1016/j.eja.2008.10.004

Campi, P., Palumbo, A.D., Mastrorilli, M., 2012. Evapotranspiration estimation of crops protected by windbreak in a Mediterranean region. Agricultural Water Management 104, 153-162. https://doi.org/10.1016/j.agwat.2011.12.010

Cleugh, H.A., 1998. Effects of windbreaks on airflow, microclimates and crop yields. Agroforestry Systems 41, 55-84.

Dufkova, J., 2007. Determination of wind erosion next to shelterbelts. Acta Universitatis Agriculturae et Silviculturae Mendelianae Brunensis, 55(5), 65-70.

Forman, R.T., Baudry, J., 1984. Hedgerows and hedgerow networks in landscape ecology. Environ. Manag. 8, 495-510. https://doi.org/10.1007/BF01871575

Gagarin, E., 1949. Holzanbau zum Schutz der Felder Rußlands. Forstwirtschaftliches Zentralblatt.

Gerersdorfer, T., Eitzinger, J., Bahrs, E., Brandenburg, C., 2010. Der Beitrag von Landschaftsstrukturen (zB Windschutzhecken) zur Ertragssituation im Ackerbau in Ostösterreich. Berichte des Meteorologischen Instituts der Albert-Ludwigs-Universität Freiburg, 32.

Hanming, H.E., Lei, Y., Lihua, Z., Han, W., Liming, F., Yong, X., Chengyun, L., 2012. The temporal-spatial distribution of light intensity in maize and soybean intercropping systems. J. Resour. Ecology 3(2), 169-173. https://doi.org/10.5814/j.issn.1674-764x.2012.02.009

He, Y., Jones, P.J., Rayment, M., 2017. A simple parameterisation of windbreak effects on wind speed reduction and resulting thermal benefits to sheep. Agricultural Forest Meteorology 239, 96-107. https://doi.org/10.1016/j.agrformet.2017.02.032

Heisler, G.M., Dewalle, D.R., 1988. 2. Effects of windbreak structure on wind flow. Agriculture, Ecosystems Environment 22, 41-69. https://doi.org/10.1016/0167-8809(88)90007-2

Kanzler, M., Böhm, C., Mirck, J., Schmitt, D., Veste, M., 2019. Microclimate effects on evaporation and winter wheat (*Triticum aestivum* L.) yield within a temperate agroforestry system. Agroforestry Systems 93, 1821-1841. https://doi.org/10.1007/s10457-018-0289-4

Kort, J., 1988. Benefits of windbreaks to field and forage crops. Agriculture, Ecosystems Environ. 22, 165-190.

Ma, R., Li, J., Ma, Y., Shan, L., Li, X., Wei, L., 2019. A wind tunnel study of the airflow field and shelter efficiency of mixed windbreaks. Aeolian Res. 41, 100544. https://doi.org/10.1016/j.aeolia.2019.100544

Miri, A., Maleki, S., Middleton, N., 2021. An investigaation into climatic and terrestrial drivers of dust storms in the Sistan region of Iran in the early twenty-first century. Science Total Environ. 757. https://doi.org/10.1016/j.scitotenv.2020.143952

Ouda, S.A., El Mesiry, T., Abdallah, E.F., Gaballah, M.S., 2007. Effect of water stress on the yield of soybean and maize grown under different intercropping patterns. Australian J. Basic Applied Sci. 1(4), 578-585.

Peri, P., Bloomberg, L., Bloomberg, M., 2002. Windbreaks in southern Patagonia, Argentinia: A review of research on growth models, windspeed reduction, and effects on crops. Agroforestry Systems 56, 129-144. https://doi.org/10.1023/A:1021314927209

Radke, J.K., Hagstrom, R.T., 1976. Strip intercropping for wind protection. Multiple Cropping 27, 201-222. https://doi.org/10.2134/asaspecpub27.c10

Řeháček, D., Khel, T., Kučera, J., Vopravil, J., Petera, M., 2017. Effect of windbreaks on wind speed reduction and soil protection against wind erosion. Soil Water Res. 12(2). https://doi.org/10.17221/45/2016-SWR

Stahr, M., 2017. Einfluss einer Hecke auf das angrenzende Mikroklima und die Ertragswirksamkeit bei Sommergerste im ökologischen Landbau im Marchfeld der Vegetationsperiode 2016. Master Thesis: University of Applied Life Sciences (BOKU), Vienna.

Sudmeyer, R.A., Speijers, J., 2007. Influence of windbreak orientation, shade and rainfall interception on wheat and lupin growth in the absence of below-ground competition. Agroforestry Systems 71, 201-214. https://doi.org/10.1007/s10457-007-9070-9

Thevs, N., Strenge, E., Aliev, K., Eraaliev, M., Lang, P., Baibagysov, A., Xu, J., 2017. Tree shelterbelts as an element to improve water resource management in Central Asia. Water 9(11), 842. https://doi.org/10.3390/w9110842

Vacek, Z., Rehácek, D., Cukor, J., Vacek S., Khel, T., Sharma, R., *et al.*, 2018. Windbreak efficiency in agricultural landscape of the Central Europe: Multiple approaches to wind erosion control. Environ. Manag. 942-954. https://doi.org/10.1007/s00267-018-1090-x

Vanneste, T., Govaert, S., Spicher, F., Brunet, J., Cousins, S., Decocq, G., *et al.*, 2020. Contrasting microclimates among hedgerows and woodlands across temperate Europe. (Elsevier, Hrsg.) Agric. Forest Meteorology 281. https://doi.org/10.1016/j.agrformet.2019.107818

Veste, M., Littmann, T., Kunneke, A., Du Toit, B., Seifert, T., 2020. Windbreaks as part of climate-smart landscapes reduce evapotranspiration in vineyards, Western Cape Province, South Africa. Plant, Soil Environ. 66(3). https://doi.org/10.17221/616/2019-PSE

Wendt, H., 1951. Der Einfluss der Hecken auf den landwirtschaflichen Ertrag. Archive for Scientific Geography (Erdkunde), 115-124.

Weninger, T., Scheper, S., Lackóová, L., Kitzler, B., Gartner, K., King, N., *et al.*, 2021. Ecosystem services of tree windbreaks in rural landscapes – a systematic review. Environmental Research Letters 1-19.

Weninger, T., Gartner, K., Riedel, S., Scheper, S., Michel, K., 2022. Der windschutzeffekt von bodenschutzanlagen am beispiel marchfeld. Österreichische Wasser-und Abfallwirtschaft 74(5), 251-257. https://doi.org/10.1007/s00506-022-00851-y